

Pulsed Hydrogen Exchange and Electrospray Charge-State Distribution as Complementary Probes of Protein Structure in Kinetic Experiments: Implications for Ubiquitin Folding[†]

Jingxi Pan, Derek J. Wilson, and Lars Konermann*

Department of Chemistry, The University of Western Ontario, London, Ontario, N6A 5B7, Canada

Received March 29, 2005; Revised Manuscript Received April 30, 2005

ABSTRACT: The possible involvement of “hidden” kinetic intermediates in the apparent two-state folding of some proteins is currently a matter of debate. This study uses time-resolved electrospray ionization (ESI) mass spectrometry with on-line pulsed hydrogen–deuterium exchange (HDX) for monitoring the refolding of acid/methanol-denatured ubiquitin. It is demonstrated that the ESI charge-state distribution (CSD) and the extent of HDX represent nonredundant probes of the protein structure in solution. When considered in isolation, the data provided by both of these probes are consistent with a two-state behavior, involving only denatured ubiquitin *D* and refolded protein *F*. However, a careful comparison of the CSD and HDX kinetics reveals the presence of an additional species, exhibiting a CSD like the folded protein but showing non-native HDX characteristics. This kinetic intermediate, *D*^{*}, is in rapid equilibrium with *D*, such that the overall reaction is consistent with the mechanism $D \leftrightarrow D^* \rightarrow F$. The results of this work suggest that the occurrence of transient intermediates may be more widespread than commonly thought, especially in cases where a cursory analysis indicates two-state behavior.

Numerous denatured proteins can spontaneously fold into their native conformations once they are exposed to favorable solvent conditions (1). Despite a lot of recent progress, many aspects regarding the kinetics of these folding processes are still not fully understood (2–5). In particular, the role of transient folding intermediates remains controversial. A large body of experimental work is consistent with the view that folding proceeds through a series of increasingly natively like structures (6–11). These folding pathways can be interpreted as one-dimensional projections of multidimensional energy landscapes (8, 12, 13). Interestingly, however, a considerable number of proteins fold in an apparent two-state fashion, i.e., without any detectable intermediates (14–17). This observation could indicate that kinetic intermediates are not a requirement for the successful folding of polypeptide chains. Instead, intermediates might correspond to kinetic traps on energy landscapes of the protein, thus representing an impediment to folding (11, 18–20). However, it has been argued that even cooperative folding events can be based on incremental assembly processes, involving a series of “hidden” intermediates. In fact, there is experimental support for the occurrence of weakly populated kinetic intermediates for a number of apparent two-state folders (21–25). The difficulties of observing these species experimentally may be due to the low stability of partially folded structures en route to the native state (26–28). Another point to consider is that many of the commonly used optical techniques, such

as circular dichroism (CD)¹ or Trp fluorescence spectroscopy, cannot provide detailed insights into the structural changes taking place during folding. Also, the very short lifetimes of many folding intermediates represents significant problems. Although the application of ultra-rapid mixing and temperature-jump experiments is becoming more and more common (5, 29), the interpretation of submillisecond signal changes is not always straightforward. Early events occurring on this time scale can indicate the rapid formation of partially folded species. Alternatively, they may reflect a response of the unfolded state to an altered solvent environment, analogous to the behavior seen for nonfoldable polymers (30, 31).

Ubiquitin is an interesting model system for addressing questions related to apparent two-state folding. The native state of this 76-residue protein (MW 8565 Da) exhibits an unusually rigid backbone structure, involving a five-stranded β sheet, two short α helices, and seven turns (32, 33). Ubiquitin plays a key role for regulating intracellular protein degradation (34). Because of the lack of suitable spectroscopic probes in the wild-type protein, many kinetic experiments have been carried out on a F45W mutant (35). Several stopped-flow fluorescence studies suggest that the refolding of GuHCl-denatured ubiquitin involves an early intermediate (35–37). Support for the occurrence of an intermediate species also comes from NMR-based hydrogen/deuterium exchange (HDX) studies on the wild-type protein (38), temperature-jump unfolding experiments (39), and recent work employing electrospray ionization mass spectrometry (ESI–MS) under equilibrium conditions (40). A number of

[†] This work was supported by the Natural Sciences and Engineering Research Council of Canada (NSERC), the Canada Foundation for Innovation (CFI), The Province of Ontario, and the Canada Research Chairs Program.

* To whom correspondence should be addressed. Telephone: (519) 661-2111 ext. 86313. Fax: (519) 661-3022. E-mail: konerman@uwo.ca. <http://publish.uwo.ca/~konerman>.

¹ Abbreviations: CD, circular dichroism; CSD, charge-state distribution; ESI, electrospray ionization; HDX, hydrogen/deuterium exchange; GuHCl, guanidinium hydrochloride; MS, mass spectrometry; NMR, nuclear magnetic resonance.

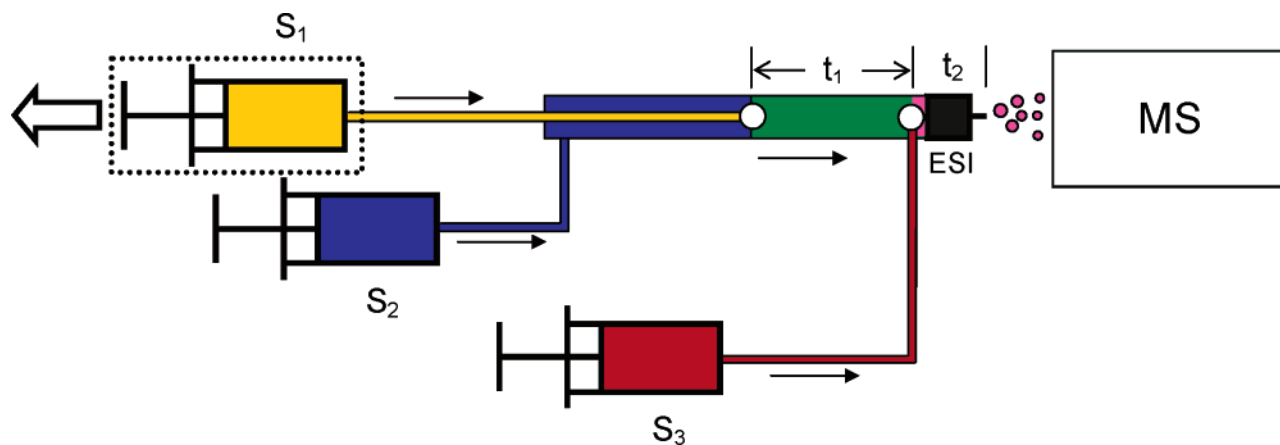


FIGURE 1: Double mixing setup for time-resolved ESI-MS with on-line pulsed HDX. Solid arrows indicate the direction of liquid flow, and white spheres represent mixers. The plungers of the three syringes are advanced simultaneously by syringe pumps. Solutions from S_1 and S_2 are mixed to trigger ubiquitin refolding at pH 10.0. Isotopic pulse labeling is initiated after a variable time period t_1 by mixing with MeOD/D₂O from S_3 , resulting in a total flow rate of 100 $\mu\text{L}/\text{min}$ at pD 10.0. Refolding times cited in the text correspond to $t_1 + t_2$, where $t_2 = 25$ ms is the (fixed) duration of the labeling pulse. S_1 is mounted on a stepper motor, thus allowing t_1 to be changed continuously.

other studies, however, have concluded that a simple two-state model is adequate for describing the folding kinetics of ubiquitin under a wide range of conditions (41–43).

In this work, we study the kinetic mechanism of ubiquitin folding by using ESI-MS in conjunction with a continuous-flow rapid-mixing device. Our laboratory has previously used similar approaches for monitoring conformational transitions of proteins in a time-resolved manner (44, 45). The charge-state distributions (CSDs) of protein ions in ESI-MS represent a highly sensitive probe of the solution-phase polypeptide conformation (46). A major determinant of these CSDs appears to be the overall compactness of the polypeptide structure, such that unfolded conformations favor the formation of higher charge states (47, 48). Individual conformational states are usually associated with distinct bell-shaped CSDs (46, 49, 50). The current study employs a variation of a previously described setup (51), designed to carry out two sequential mixing steps. This system allows an initially denatured protein to be exposed to refolding conditions for a variable amount of time. Subsequently, an HDX labeling pulse is initiated by exposing the protein to a deuterated solvent under rapid exchange conditions. During this step, hydrogens in amide groups and amino acid side chains undergo HDX in a structurally sensitive manner. Largely unfolded proteins will show high exchange levels, whereas a stable intramolecular hydrogen-bonding network and/or the steric protection of exchangeable sites will reduce the extent of HDX (47, 52, 53). Ubiquitin has 144 exchangeable hydrogen atoms, 72 of which are located in the amide backbone (52). The labeling pulse is terminated after a fixed amount of time by protein desolvation during ESI. The technique employed here is conceptually related to traditional MS-based quench-flow experiments (8–10, 54). However, because of the quasi-instantaneous MS analysis of the proteins after labeling used here, the protein compactness (on the basis of the CSD information) can be directly correlated with the HDX behavior of coexisting conformational species. Consequently, two probes are available that simultaneously report on different aspects of the protein structure during folding (55, 56).

The native conformation of ubiquitin breaks down in acidic solutions containing organic cosolvents such as methanol.

The resulting denatured state has been extensively characterized by NMR methods (32). It was found to exhibit a highly dynamic structure that retains natively like elements in the N-terminal region, namely, a two-stranded antiparallel β sheet and a central α helix. In contrast, the C-terminal region of the protein undergoes a transition from a β -sheet structure to one that preferentially samples non-native α -helical conformations. Several ESI-MS-based studies have explored conformational transitions involving acid/methanol-denatured ubiquitin under equilibrium conditions (40, 52, 57). However, there appears to be very little information on the kinetic folding mechanism of this species.

The experimental approach used here reveals a very interesting phenomenon. When considered in isolation, both the measured CSDs and the HDX behavior of ubiquitin are consistent with a two-state folding mechanism. However, a side-by-side comparison of the data provided by the two structural probes reveals the presence of a third species. This study, therefore, provides an example of how kinetic intermediates may be identified by using techniques that provide complementary information on structural changes taking place during folding.

EXPERIMENTAL PROCEDURES

Chemicals. Wild-type bovine ubiquitin (Sigma, St. Louis, MO), bradykinin (Bachem AG, Bubendorf, Switzerland), deuterium oxide and ammonium deuterioxide (Cambridge Isotope Laboratories, Andover, MA), methyl alcohol-*d* (Aldrich, Milwaukee, WI), methanol and hydrochloric acid (Caledon Laboratories, Georgetown, ON, Canada), and ammonium hydroxide (Fisher Scientific, Nepean, ON, Canada) were used without further purification. Solution pH and pD values were measured using an accumet pH meter (Fisher Scientific).

Time-Resolved ESI-MS. The double mixing setup used for this study is depicted in Figure 1. The plungers of syringes S_1 , S_2 , and S_3 are advanced simultaneously by syringe pumps (Harvard Apparatus, model 22, Saint Laurent, PQ, Canada). Solutions from S_1 [100 μM acid-denatured ubiquitin in water/methanol (50:50, v/v, pH 2.0) at 10 $\mu\text{L}/\text{min}$] and S_2 [NH_4OH in water/methanol (50:50, v/v) with

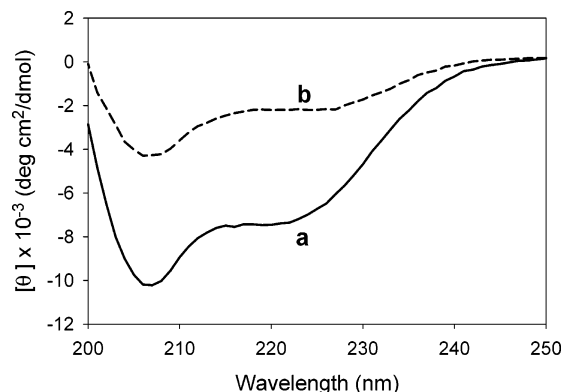


FIGURE 2: CD spectra of 20 μM ubiquitin in 50% methanol. (a) Denatured protein at pH 2.0. (b) Refolded protein at pH 10.0.

30 μM bradykinin at 10 $\mu\text{L}/\text{min}$] are mixed near the end of the inner capillary to trigger refolding at pH 10.0. Pulse labeling is initiated after a variable time period t_1 by mixing with $\text{MeOD}/\text{D}_2\text{O}$ (50:50, v/v) from S_3 , resulting in a total flow rate of 100 $\mu\text{L}/\text{min}$ at pD 10.0 and a final protein concentration of 10 μM . Subsequently, the reaction mixture is electrosprayed for mass analysis. The refolding times cited in the text correspond to $t_1 + t_2$, where $t_2 = 25$ ms is the duration of the labeling pulse. S_1 is mounted on a stepper motor, thus allowing the position of the first mixer to be changed continuously. Efficient mixing with this type of apparatus has been demonstrated previously, and laminar flow effects were accounted for as described (51). The use of alkaline conditions for labeling is necessitated by the requirement for intrinsic HDX rate constants in the range of 10^3 s^{-1} (58). It is noted that the $\text{CH}_3\text{-OD}$ content of the solutions used may lead to intrinsic HDX rates that are somewhat lower than those expected in pure D_2O . However, it will be seen that the HDX levels incurred by the protein during the 25 ms labeling period are sufficient for the purpose of this work. The use of a constant pH (or pD) throughout the double mixing sequence avoids potential artifacts associated with changes of the solution conditions during labeling (59). Bradykinin in syringe S_2 serves as an internal standard to ensure constant labeling conditions for the different time points studied. All labile hydrogens in this 9 amino acid peptide are accessible to the solvent and thus readily exchangeable (52). Mass spectra were recorded on a Micromass/Waters LCT time-of-flight mass spectrometer at a cone voltage of 40 V and a capillary voltage of 5000 V. The presence of high methanol concentrations in the reaction mixture for the current experiments undoubtedly facilitated the acquisition of kinetic data with a high signal-to-noise ratio. However, it is pointed out that this aspect does not represent an inherent limitation of the method employed here, because similar on-line experiments can also be carried out in the absence of organic cosolvents (55).

RESULTS AND DISCUSSION

Ubiquitin was initially denatured by exposing it to methanol/water (50:50, v/v) at pH 2.0. The CD spectrum obtained under these conditions is in agreement with data obtained previously (52) (Figure 2). Refolding was triggered by mixing with ammonia solution, resulting in a pH jump to 10.0, at a constant methanol concentration. The dramatic change in the CD signature upon refolding is

consistent with the loss of non-native α -helical structure (32) (Figure 2). The CD spectrum of refolded ubiquitin is indistinguishable from that of the native protein (data not shown).

Denatured ubiquitin shows an ESI mass spectrum that is characterized by a broad CSD with a maximum around 11+ (Figure 3A). Consistent with earlier work (40, 51), mass spectra acquired during refolding have a bimodal appearance. They exhibit a relatively broad CSD centered at 9+, and a more narrow one encompassing the 6+ and 5+ charge states (parts B–D of Figure 3). Refolding of the protein is reflected in a gradual intensity decrease of the highly charged protein ions and a concomitant increase of the 6+ and 5+ ions. The initial CSD shift from 11+ to 9+ (parts A and B of Figure 3) may indicate a conformational change taking place during the dead time of the experiment. Alternatively, this effect could result from the different ionization conditions used (pD 10.0 versus pH 2.0), which might lead to reduced charge acquisition during ESI.

The mass distributions obtained after pulsed HDX can be grouped in two categories. Protein ions in charge states from 13+ to 7+ exhibit unimodal distributions, with maxima that are shifted 83 ± 4 Da relative to unlabeled ubiquitin. As an example, Figure 3 shows data recorded for the 9+ charge state (parts E–G of Figure 3, blue dashed lines). A different behavior is observed for the 6+ and 5+ ions. For times longer than ca. 100 ms, the corresponding peaks show bimodal mass distributions (parts E–G of Figure 3, red lines). The low mass portion of these distributions shows a shift of 58 ± 2 Da, whereas the high mass portion coincides with the distribution observed for the 13+ to 7+ charge states. From these data, two distinct kinetic species are easily identified. A denatured conformation D is associated with the CSD peaking at 9+ and a high HDX level. Refolded ubiquitin F corresponds to the 6+/5+ charge states and a low HDX level. It is interesting to note the different half widths of the high and low mass peaks, 27 ± 2 versus 16 ± 2 Da, which reflect the greater conformational heterogeneity of the denatured protein (60).

When considered in isolation, both the CSDs in parts B–D of Figure 3 and the mass distributions in parts E–G of Figure 3 are consistent with a two-state process $D \rightarrow F$. However, a careful comparison of the information provided by the two structural probes reveals a more complex mechanism. For a two-state scenario, the occurrence of a bimodal CSD should *always* be correlated with a bimodal mass distribution. Inspection of the data in Figure 3 reveals that such a correlation exists only for longer reaction times. In contrast, the bimodal CSD observed immediately after initiation of refolding is associated with a unimodal mass distribution, corresponding to a high HDX level (parts B and E of Figure 3). This observation reveals the presence of an additional species, denoted as D^* , that is associated with the 6+/5+ charge states and that exhibits a high HDX level. The fact that D and D^* show HDX characteristics that are virtually indistinguishable suggests that the two species undergo rapid interconversion during the labeling pulse (61). This implies that D and D^* are separated by a relatively low energy barrier. In contrast, the transition to F occurs on a slower time scale, which is indicative of a major barrier. A schematic depiction of a reaction mechanism that is consistent with these results is given in Figure 4.

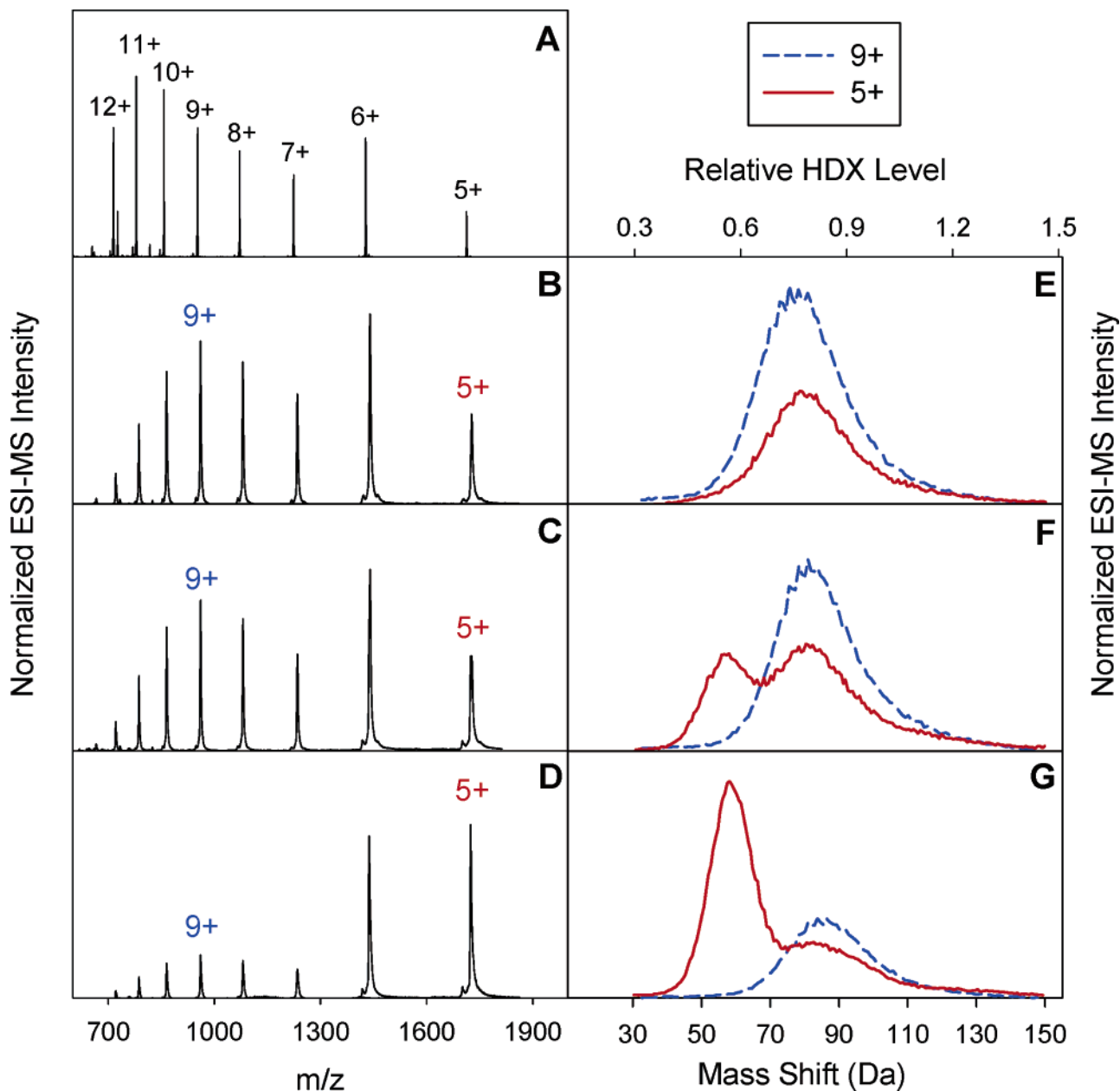


FIGURE 3: ESI mass spectra of ubiquitin in 50% methanol. (A) Denatured protein at pH 2.0. (B, C, and D) Time-resolved spectra, recorded 40 ms, 240 ms, and 3.3 s, respectively, after a jump from pH 2.0 to pD 10.0. Close-up views of the 5+ and 9+ charge states for the same three time points are depicted in E–G. The x axes in E–G display the mass shift relative to unlabeled ubiquitin and the relative HDX level, given by (mass shift)/(144 \times 0.712). The factor 0.712 takes into account the isotopic composition of the labeling solution and back exchange in the ion source; the factor was determined from the HDX level of the internal standard bradykinin (52).

Additional support for the proposed three-state mechanism is provided by intensity–time profiles of the individual ionic signals. The intensity of the 5+ charge state, when integrated over its entire mass distribution, reflects the formation of F as well as the depletion of D^* (D is not expected to affect this charge state to a large extent). The compensating nature of the D^* and F contributions leads to an overall signal change that is quite small, from 0.66 to 1.0 (pink trace in Figure 5). A much larger change, from 0.26 to 1.0, is observed when monitoring only the low mass portion of the 5+ charge state (red), which exclusively reflects the formation of F . Also shown in Figure 5 is the profile of the 9+ charge state, integrated over its entire mass distribution (blue), which reports on the depletion of D . The profiles in Figure 5, as well as those of the other charge states (not shown), exhibit single-exponential behavior with $k_{\text{obs}} =$

(1.3 \pm 0.1) s^{-1} . It is realized that our data do not provide direct proof of the on-pathway nature of D^* , because the kinetic model proposed in Figure 4 is kinetically equivalent to a mechanism where the positions of D and D^* are reversed (8, 9, 36).

As mentioned earlier, NMR studies have led to a structural model of acid/methanol-denatured ubiquitin that involves three distinct elements, namely, an N-terminal β sheet, a short central helix, and a long helical segment in the C-terminal region. According to Figure 5 in the work of Brutscher et al. (32), these three elements preferentially adopt a largely extended arrangement. Given the very dynamic nature of the denatured protein, it is easy to imagine fluctuations between this extended structure and more compact arrangements where the three elements are in closer contact with each other. Changes of a few torsional angles in the highly flexible

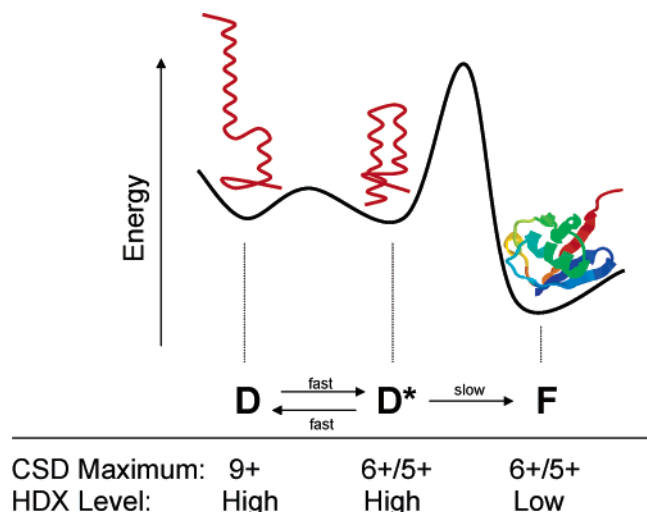


FIGURE 4: Schematic depiction of a three-state mechanism for ubiquitin folding. Kinetic effects because of X-Pro cis/trans isomerization are not considered.

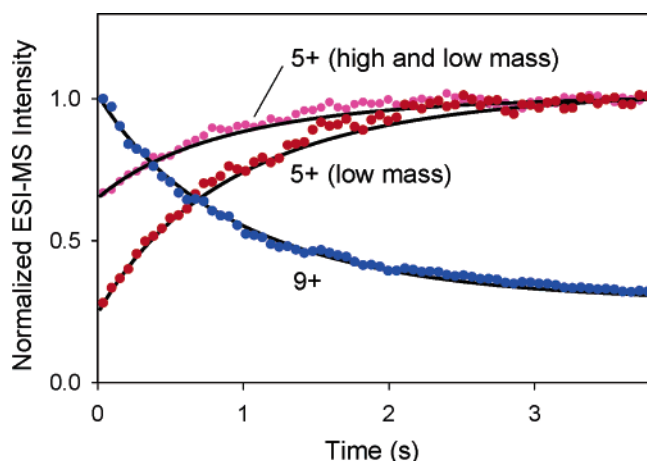


FIGURE 5: Kinetic ESI-MS profiles measured during ubiquitin folding with pulsed HDX. Solid lines are exponential fits to the data. See the text for details.

linker regions (residues 18–22 and 35–38) would be sufficient to bring about structural transitions of this kind. We hypothesize that fluctuations of this type might provide the basis of the rapid $D \leftrightarrow D^*$ interconversion observed in the current work. According to the CSDs of the two species, D corresponds to more extended structures, whereas D^* comprises more compact conformations. Notably, a three-state folding mechanism like that found in this work has also been proposed for GuHCl-denatured ubiquitin (36). This finding is interesting, because the structural features of the denatured protein under those conditions are expected to be quite different from those encountered in this work (unlike methanol, GuHCl does not induce non-native α -helical structures).

The persistence of a significant population of unfolded proteins toward the end of the experimental time window (parts D and G of Figure 3 and Figure 5) indicates the presence of a subpopulation of slow-folding polypeptide chains. Previous work has ascribed this behavior to the occurrence of non-native cis proline isomers in these protein molecules (42). Native ubiquitin contains three trans prolines in positions 19, 37, and 38. Denaturation of the protein significantly relaxes existing steric constraints, such that a

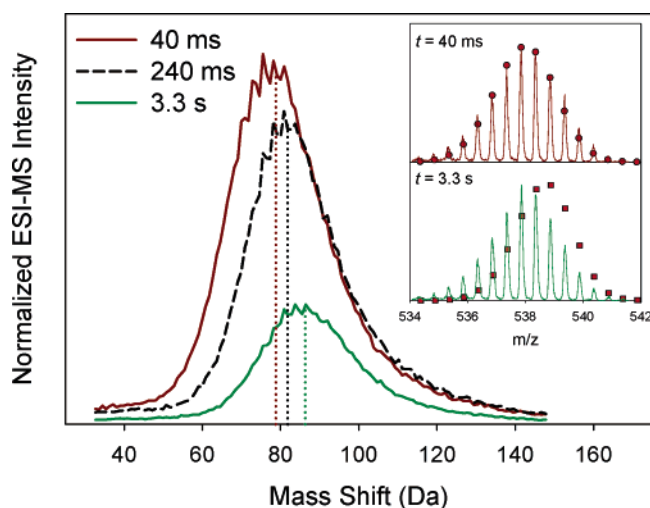


FIGURE 6: Close-up view of the ubiquitin 9+ ionic signal after pulsed HDX, obtained for refolding times of $t = 40$ ms, 240 ms, and 3.3 s. As for all experiments in this work, the duration of the labeling pulse was kept constant at 25 ms. Vertical dotted lines indicate the centroids of the three signals, 79, 82, and 86 Da, respectively. The mass shifts measured for $t = 40$ ms and 3.3 s differ by $\sim 10\%$. (Inset) Isotope distributions of the internal standard bradykinin after pulsed HDX, obtained for refolding times of $t = 40$ ms (upper) and $t = 3.3$ s (lower). The two spectra of the doubly charged ion are virtually indistinguishable. The bradykinin spectrum for $t = 40$ ms is well-described by a modeled isotope distribution, assuming an HDX probability of 0.712 (upper, red circles). The distribution modeled in the lower inset (red squares) assumes an HDX probability of 0.780, corresponding to a 10% increase in the labeling level. This distribution does *not* match the measured spectrum of the internal standard. This control experiment confirms that the $\sim 10\%$ difference in mass shift observed for the ubiquitin 9+ ions for labeling times of 40 ms and 3.3 s is not an experimental artifact.

certain percentage of these residues can undergo isomerization. When placing the protein under refolding conditions, only those polypeptide chains that have all prolines in the correct orientation fold rapidly, in the present case with an overall rate constant of ~ 1.3 s $^{-1}$ (62, 63). This scenario implies that the relative proportion of denatured proteins containing cis prolines should increase during the first few seconds of the reaction. Such a view is consistent with a notable increase of the HDX level observed for highly charged ubiquitin ions with increasing refolding time (Figure 6). Although all three Pro residues are located in the linker regions of the model proposed by Brutscher et al. (32), it appears that the higher labeling levels detected toward the end of the experimental time window are due to structural perturbations in the denatured protein, caused by the presence of cis prolines. In the present case, the average HDX level incurred by the denatured protein after pulse labeling increases from 79 to 86 Da during the experimental time window. The labeling behavior of the internal standard bradykinin clearly confirms that this $\sim 10\%$ increase is *not* attributable to an experimental artifact, e.g., a potential change in HDX conditions for different time points (inset of Figure 6).

CONCLUSIONS

The experiments described in this study show that a process exhibiting many of the hallmarks of two-state folding (single-exponential kinetics, bimodal charge, and HDX

distributions) can still involve a clearly observable intermediate. Here, the existence of such a species was uncovered by employing HDX and CSD as complementary structural probes. D and D^* are indistinguishable based on their HDX behaviors, whereas the measured CSDs do not allow a differentiation of D^* and F . Thus, the intermediate would have gone undetected in kinetic experiments relying on only one of these probes. These results are in line with the notion that the occurrence of folding intermediates is more widespread than commonly thought, especially in cases where a cursory analysis indicates a two-state behavior (21–24). It will be interesting to see if results similar to those described in this work will be found when applying time-resolved ESI–MS with on-line pulsed HDX to other apparent two-state folders.

REFERENCES

- Anfinsen, C. B. (1973) Principles that govern the folding of protein chains, *Science* 181, 223–230.
- Onuchic, J. N., and Wolynes, P. G. (2004) Theory of protein folding, *Curr. Opin. Struct. Biol.* 14, 70–75.
- Kubelka, J., Hofrichter, J., and Eaton, W. A. (2004) The protein folding “speed limit”, *Curr. Opin. Struct. Biol.* 14, 76–88.
- Daggett, V., and Fersht, A. (2003) The present view of the mechanism of protein folding, *Nat. Rev. Mol. Cell Biol.* 4, 497–502.
- Welker, E., Maki, K., Shastry, M. C. R., Juminaga, D., Bhat, R., Scheraga, H. A., and Roder, H. (2004) Ultrarapid mixing experiments shed new light on the characteristics of the initial conformational ensemble during the folding of ribonuclease A, *Proc. Nat. Acad. Sci. U.S.A.* 101, 17681–17686.
- Roder, H., Elöve, G. A., and Englander, S. W. (1988) Structural characterization of folding intermediates in cytochrome *c* by H-exchange labelling and proton NMR, *Nature* 335, 700–704.
- Jemth, P., Gianni, S., Day, R., Li, B., Johnson, C. M., Daggett, V., and Fersht, A. R. (2004) Demonstration of a low-energy on-pathway intermediate in a fast-folding protein by kinetics, protein engineering, and simulation, *Proc. Nat. Acad. Sci. U.S.A.* 101, 6450–6455.
- Heidary, D. K., Gross, L. A., Roy, M., and Jennings, P. A. (1997) Evidence for an obligatory intermediate in the folding of Interleukin-1b, *Nat. Struct. Biol.* 4, 725–731.
- Tsui, V., Garcia, S., Cavagnero, S., Siuzdak, G., Dyson, H. J., and Wright, P. E. (1999) Quench-flow experiments combined with mass spectrometry show apomyoglobin folds through an obligatory intermediate, *Protein Sci.* 8, 45–49.
- Miranker, A., Robinson, C. V., Radford, S. E., Aplin, R., and Dobson, C. M. (1993) Detection of transient protein folding populations by mass spectrometry, *Science* 262, 896–900.
- Krishna, M. M. G., Lin, Y., and Englander, S. W. (2004) Protein misfolding: Optional barriers, misfolded intermediates, and pathway heterogeneity, *J. Mol. Biol.* 343, 1095–1109.
- Dill, K. A. (1999) Polymer principles and protein folding, *Protein Sci.* 8, 1166–1180.
- Pande, V. S., Grosberg, A. Y., Tanaka, T., and Rokhsar, D. S. (1998) Pathways for protein folding: Is a “new view” needed? *Curr. Opin. Struct. Biol.* 8, 68–79.
- Plaxco, K. W., Simons, K. T., Ruczinski, I., and Baker, D. (2000) Topology, stability, sequence, and length: Defining the determinants of two-state protein folding kinetics, *Biochemistry* 39, 11177–11183.
- Makarov, D. E., Keller, C. A., Plaxco, K. W., and Metiu, H. (2002) How the folding rate constant of simple, single-domain protein depends on the number of native contacts, *Proc. Natl. Acad. Sci. U.S.A.* 99, 3535–3539.
- Miller, E. J., Fischer, K. F., and Marqusee, S. (2002) Experimental evaluation of topological parameters determining protein-folding rates, *Proc. Natl. Acad. Sci. U.S.A.* 99, 10359–10363.
- Makarov, D., and Plaxco, K. W. (2003) The topomer search model: A simple, quantitative theory of two-state protein folding kinetics, *Protein Sci.* 12, 17–26.
- Dill, K. A., and Chan, H. S. (1997) From Levinthal to pathways to funnels, *Nat. Struct. Biol.* 4, 10–19.
- Socci, N. D., Onuchic, J. N., and Wolynes, P. G. (1998) Protein folding mechanisms and the multidimensional folding funnel, *Proteins: Struct., Funct., Genet.* 32, 136–158.
- Sosnick, T. R., Mayne, L., Hiller, R., and Englander, S. W. (1994) The barriers in protein folding, *Nat. Struct. Biol.* 1, 149–156.
- Bachmann, A., and Kiefhaber, T. (2001) Apparent two-state tandemistat folding is a sequential process along a defined route, *J. Mol. Biol.* 306, 375–386.
- Sanchez, I. E., and Kiefhaber, T. (2003) Evidence for sequential barriers and obligatory intermediates in apparent two-state protein folding, *J. Mol. Biol.* 325, 367–376.
- Feng, H., Takei, J., Lipsitz, R., Tjandra, N., and Bai, Y. (2003) Specific non-native hydrophobic interactions in a hidden folding intermediate: Implications for protein folding, *Biochemistry* 42, 12461–12465.
- Fersht, A. R. (2000) A kinetically significant intermediate in the folding of barnase, *Proc. Nat. Acad. Sci. U.S.A.* 97, 14121–14126.
- Korzhev, D. M., Salvatella, X., Vendruscolo, M., Di Nardo, A. A., Davidson, A. R., Dobson, C. M., and Kay, L. E. (2004) Low-populated folding intermediates of Fyn SH3 characterized by relaxation dispersion NMR, *Nature* 430, 586–590.
- Baldwin, R. L., and Rose, G. D. (1999) Is protein folding hierarchic? I. Local structure and peptide folding, *Trends Biol. Sci.* 24, 26–33.
- Baldwin, R. L., and Rose, G. D. (1999) Is protein folding hierarchic? II. Folding intermediates and transition states, *Trends Biol. Sci.* 24, 77–83.
- Bai, Y. (2003) Hidden intermediates and Levinthal paradox in the folding of small proteins, *Biochem. Biophys. Res. Comm.* 305, 785–788.
- Yang, W. Y., and Gruebele, M. (2003) Folding at the speed limit, *Nature* 423, 193–197.
- Jennings, P. A. (1998) Speeding along the protein folding highway, are we reading the signs correctly? *Nat. Struct. Biol.* 5, 846–848.
- Qi, P. X., Sosnick, T. R., and Englander, S. W. (1998) The burst phase in ribonuclease A folding and the solvent dependence of the unfolded state, *Nat. Struct. Biol.* 5, 882–884.
- Brutscher, B., Brüchweiler, R., and Ernst, R. R. (1997) Backbone dynamics and structural characterization of the partially folded A state of ubiquitin by ^1H , ^{13}C , and ^{15}N nuclear magnetic resonance spectroscopy, *Biochemistry* 36, 13043–13053.
- Vijay-Kumar, S., Bugg, C. E., and Cook, W. J. (1987) Structure of ubiquitin refined at 1.8 Å resolution, *J. Mol. Biol.* 194, 531–544.
- Carrano, A. C., Eytan, E., Hershko, A., and Pagano, M. (1999) SKP2 is required for ubiquitin-mediated degradation of the CDK inhibitor p27, *Nat. Cell Biol.* 1, 193–199.
- Khorasanizadeh, S., Peters, I. D., Butt, T. R., and Roder, H. (1993) Folding and stability of a tryptophan-containing mutant of ubiquitin, *Biochemistry* 32, 7054–7063.
- Khorasanizadeh, S., Peters, I. D., and Roder, H. (1996) Evidence for a three-state model of protein folding from kinetic analysis of ubiquitin variants with altered core residues, *Nat. Struct. Biol.* 3, 193–205.
- Went, H. M., Benitez-Cardoza, C. G., and Jackson, S. E. (2004) Is an intermediate state populated on the folding pathway of ubiquitin? *FEBS Lett.* 567, 333–338.
- Briggs, M. S., and Roder, H. (1992) Early hydrogen-bonding events in the folding reaction of ubiquitin, *Proc. Natl. Acad. Sci. U.S.A.* 89, 2017–2021.
- Chung, H. S., Khalil, M., Smith, A. W., Ganim, Z., and Tokmakoff, A. (2005) Conformational changes during nanosecond-to-millisecond unfolding of ubiquitin, *Proc. Nat. Acad. Sci. U.S.A.* 102, 612–617.
- Dobo, A., and Kaltashov, I. A. (2001) Detection of multiple protein conformational ensembles in solution via deconvolution of charge-state distributions in ESI–MS, *Anal. Chem.* 73, 4763–4773.
- Krantz, B. A., Moran, L. B., Kentsis, A., and Sosnick, T. R. (2000) D/H amide kinetic isotope effects reveal when hydrogen bonds form during protein folding, *Nat. Struct. Biol.* 7, 62–71.
- Krantz, B. A., and Sosnick, T. R. (2000) Distinguishing between two-state and three-state models for ubiquitin folding, *Biochemistry* 39, 11696–11701.
- Sosnick, T. R., Dothager, R. S., and Krantz, B. A. (2004) Differences in the folding transition state of ubiquitin indicated by F and Y analyses, *Proc. Nat. Acad. Sci. U.S.A.* 101, 17377–17382.

44. Simmons, D. A., Wilson, D. J., Lajoie, G. A., Doherty-Kirby, A., and Konermann, L. (2004) Subunit disassembly and unfolding kinetics of hemoglobin studied by time-resolved electrospray mass spectrometry, *Biochemistry* 43, 14792–14801.
45. Wilson, D. J., Rafferty, S. P., and Konermann, L. (2005) Kinetic unfolding mechanism of the inducible nitric oxide synthase oxygenase domain determined by time-resolved electrospray mass spectrometry, *Biochemistry* 44, in press.
46. Chowdhury, S. K., Katta, V., and Chait, B. T. (1990) Probing conformational changes in proteins by mass spectrometry, *J. Am. Chem. Soc.* 112, 9012–9013.
47. Kaltashov, I. A., and Eyles, S. J. (2002) Studies of biomolecular conformations and conformational dynamics by mass spectrometry, *Mass Spectrom. Rev.* 21, 37–71.
48. Felitsyn, N., Peschke, M., and Kebarle, P. (2002) Origin and number of charges observed on multiply protonated native proteins produced by ESI, *Int. J. Mass Spectrom. Ion Proc.* 219, 39–62.
49. Konermann, L., and Douglas, D. J. (1997) Acid-induced unfolding of cytochrome *c* at different methanol concentrations: Electrospray ionization mass spectrometry specifically monitors changes in the tertiary structure, *Biochemistry* 36, 12296–12302.
50. Grandori, R. (2002) Detecting equilibrium cytochrome *c* folding intermediates by electrospray ionization mass spectrometry: Two partially folded forms populate the molten globule state, *Protein Sci.* 11, 453–458.
51. Wilson, D. J., and Konermann, L. (2003) A capillary mixer with adjustable reaction chamber volume for millisecond time-resolved studies by electrospray mass spectrometry, *Anal. Chem.* 75, 6408–6414.
52. Katta, V., and Chait, B. T. (1993) Hydrogen/deuterium exchange electrospray ionization mass spectrometry: A method for probing protein conformational changes in solution, *J. Am. Chem. Soc.* 115, 6317–6321.
53. Krishna, M. M. G., Hoang, L., Lin, Y., and Englander, S. W. (2004) Hydrogen exchange methods to study protein folding, *Methods* 34, 51–64.
54. Pan, H., Raza, A. S., and Smight, D. L. (2004) Equilibrium and kinetic folding of rabbit muscle triosephosphate isomerase by hydrogen exchange mass spectrometry, *J. Mol. Biol.* 336, 1251–1263.
55. Simmons, D. A., and Konermann, L. (2002) Characterization of transient protein folding intermediates during myoglobin reconstitution by time-resolved electrospray mass spectrometry with on-line isotopic pulse labeling, *Biochemistry* 41, 1906–1914.
56. Simmons, D. A., Dunn, S. D., and Konermann, L. (2003) Conformational dynamics of partially denatured myoglobin studied by time-resolved electrospray mass spectrometry with online hydrogen–deuterium exchange, *Biochemistry* 42, 5896–5905.
57. Samalikova, M., and Grandori, R. (2003) Protein charge-state distributions in electrospray-ionization mass spectrometry do not appear to be limited by the surface tension of the solvent, *J. Am. Chem. Soc.* 125, 13352–13353.
58. Bai, Y., Milne, J. S., Mayne, L., and Englander, S. W. (1993) Primary structure effects on peptide group hydrogen exchange, *Proteins: Struct., Funct., Genet.* 17, 75–86.
59. Bieri, O., and Kiefhaber, T. (2001) Origin of apparent fast and non-exponential kinetics of lysozyme folding measured in pulsed hydrogen exchange experiments, *J. Mol. Biol.* 310, 919–935.
60. Konermann, L., and Simmons, D. A. (2003) Protein folding kinetics and mechanisms studied by pulse-labeling and mass spectrometry, *Mass Spectrom. Rev.* 22, 1–26.
61. Wagner, D. S., and Anderegg, R. J. (1994) Conformation of cytochrome *c* studied by deuterium exchange–electrospray ionization mass spectrometry, *Anal. Chem.* 66, 706–711.
62. Brandts, J. F., Brennan, M., and Lin, L. (1977) Unfolding and refolding occur much faster for a proline-free protein than for most proline-containing proteins, *Proc. Natl. Acad. Sci. U.S.A.* 74, 4178–4181.
63. Wedemeyer, W. J., Welker, E., and Scheraga, H. A. (2002) Proline cis–trans isomerization and protein folding, *Biochemistry* 41, 14637–14644.

BI050575E